

Geophysical Research Letters



RESEARCH LETTER

10.1029/2019GL084915

Key Points:

- Global-scale applications of satellite-radar data require measurements to be connected to an absolute geocentric reference frame
- The global network of geodetic radio telescopes provides an unexploited and novel link to unify displacement rate maps globally
- Tracking of radar satellites is easily implemented into telescope operations without impacting upon existing activities or infrastructure

Supporting Information:

- Supporting Information S1

Correspondence to:

A. L. Parker,
Amy.Parker@curtin.edu.au

Citation:

Parker, A. L., McCallum, L., Featherstone, W. E., McCallum, J. N., & Haas, R. (2019). The Potential for Unifying Global-Scale Satellite Measurements of Ground Displacements Using Radio Telescopes. *Geophysical Research Letters*, *46*, 11,841–11,849. <https://doi.org/10.1029/2019GL084915>

Received 9 AUG 2019

Accepted 13 OCT 2019

Accepted article online 1 NOV 2019

Published online 7 NOV 2019

The Potential for Unifying Global-Scale Satellite Measurements of Ground Displacements Using Radio Telescopes

A. L. Parker¹ , L. McCallum² , W. E. Featherstone¹ , J. N. McCallum², and R. Haas³

¹School of Earth and Planetary Sciences, Curtin University of Technology, Perth, WA, Australia, ²School of Natural Sciences, University of Tasmania, Hobart, TAS, Australia, ³Department of Space, Earth and Environment, Chalmers University of Technology, Onsala, Sweden

Abstract The expansion of globally consistent satellite-radar imagery presents new opportunities to measure Earth-surface displacements on intercontinental scales. Yet global applications, including a complete assessment of the land contribution to relative sea-level rise, first demand new solutions to unify relative satellite-radar observations in a geocentric reference frame. The international network of Very Long Baseline Interferometry telescopes provides an existing, yet unexploited, link to unify satellite-radar measurements on a global scale. Proof-of-concept experiments reveal the suitability of these instruments as high-amplitude reflectors for satellite radar and thus provide direct connections to a globally consistent reference frame. Automated tracking of radar satellites is easily integrated into telescope operations alongside ongoing schedules for geodesy and astrometry. Utilizing existing telescopes in this way completely avoids the need for additional geodetic infrastructure or ground surveys and is ready to implement immediately across the telescope network as a first step toward using satellite radar on a global scale.

Plain Language Summary Satellite-radar imagery is used increasingly to map Earth-surface displacements, providing unprecedented insights into geohazards and crustal changes. Although the coverage of radar imagery is now global, applications to global-scale processes are not underway. A fundamental obstacle is the need to transform satellite-based displacement maps from measuring changes relative to an arbitrary point to being constrained within a globally consistent reference frame. In a new approach, the international network of radio telescopes is shown to be a unique, unexplored, yet readily available, link, requiring no installations of additional infrastructure or ongoing fieldwork. Proof-of-concept experiments using telescopes on two continents demonstrate that these instruments simultaneously provide high-intensity reflections in satellite-radar imagery, while simultaneously acting as direct ties to a global reference frame. Automated tracking of radar satellites requires only minor additions to existing telescope operations and is therefore immediately ready to implement globally, impacting upon the rapidly growing numbers and diversity of scientists using satellite radar to address geohazards on ever-increasing scales. This is a first step toward integrating satellite-radar measurements on a global scale, which will inevitably deliver new understanding of the processes that shape Earth's crust, including a complete, consistent assessment of the contribution of land displacements to relative sea-level rise.

1. Introduction

High-resolution (down to tens of meters) ground displacement maps obtained via repeat satellite radar (interferometric synthetic aperture radar or InSAR) fulfill an increasingly significant role in deciphering the effects of solid Earth, cryospheric and anthropogenic processes that manifest as spatiotemporal changes in the height of the Earth's surface (e.g., Elliott et al., 2016; Galloway et al., 1998; Goldstein et al., 1993; Massonnet & Feigl, 1998). The spatial coverage of InSAR imagery has now evolved to a systematic global basis provided via open access by the European Space Agency's Sentinel-1 satellites (Copernicus Space Component Mission Management Team, 2017; Torres et al., 2012). Rather than local- or regional-scale applications, this provides new opportunities for InSAR to deliver complete, global-scale assessments of the processes shaping Earth's geomorphic and tectonic landscapes, including the land component of sea-level change.

©2019. American Geophysical Union. All Rights Reserved.

This is an open access article under the terms of the Creative Commons Attribution License, which permits use, distribution and reproduction in any medium, provided the original work is properly cited.

Global unification of InSAR-derived ground displacements first requires measurements on water-separated landmasses to be tied into a consistent, geocentric reference frame (e.g., Mahapatra et al., 2018). Ground displacements from InSAR are measured relative to the time of the first image acquisition and are defined with respect to some arbitrary reference frame, such as the mean displacement of the image (Finnegan et al., 2008) or the displacement of pixel(s) in a far-field region that has to be assumed to be nondeforming (Elliott et al., 2016; Schmidt & Bürgmann, 2003). As the radar scenes overlap in range and azimuth, many synthetic aperture radar (SAR) frames may be combined into a single image on regional or continental scales (Hussein et al., 2018; Walters et al., 2016). However, due to the relative nature of the measurements and time-varying scattering characteristics over water bodies, InSAR is limited to overlapping scenes on the same landmass and thus cannot be used directly on a global scale. Therefore, special strategies are necessary to overcome this deficiency, which we present here.

The transformation of InSAR measurements to a consistent reference frame is possible via connection to absolute geodetic infrastructure (e.g., continuous Global Navigation Satellite Systems—cGNSS) (Bock et al., 2012; Dheenathayalan et al., 2016), referencing the measurements to pixel(s) that are coincident with, or proximal to, such instrumentation (Bekaert et al., 2017). It is preferable to install co-located artificial corner reflectors (CRs) or actively transmitting transponders (Mahapatra et al., 2014) to (1) ensure there is interferometric coherence proximal to the cGNSS (Parker et al., 2017) and (2) avoid the assumption that the average displacement of nearby pixels is representative of that at the instrument (Raucoules et al., 2013; Wöppelmann et al., 2013) but which may not be true and cannot be verified.

However, neither CRs nor transponders are necessarily a readily global solution. Installing CRs is costly (thousands of dollars) and involves fixing the CR orientation to a single satellite and orbit direction (i.e., ascending or descending) or installing multiple CRs (e.g., Fuhrmann et al., 2018). Periodic site maintenance is then required to remove debris and assess possible disturbances or geometric alterations arising from environmental factors. Transponders are not yet commercially available and, once installed, require battery changes (Mahapatra et al., 2018) and radio transmission licenses to be operated, which are restricted in many jurisdictions (Garthwaite, 2017). If not directly and rigidly attached to the cGNSS monument, subsequent and regular repeat local ties from CRs and/or transponders to the cGNSS then require ongoing long-term repeat fieldwork at a cost.

A unique and, until now, unexplored solution to these problems is the international network of geodetic Very Long Baseline Interferometry (VLBI) radio telescopes. The global geodetic network currently consists of ~30 VLBI telescopes, with at least one located on each major landmass and over which Sentinel-1 acquires imagery at a frequency of between 1 and 12 days (Figure 1). These telescopes act simultaneously as direct ties to the International Terrestrial Reference Frame (ITRF) (Altamimi et al., 2011, 2016), while other radio telescopes (e.g., ground stations) have been identified as passive reflectors suited to radiometric calibration for SAR (Keen, 1983; Meadows, 2000; van't Klooster, 2011; Zakharov et al., 2003). Exploiting VLBI telescopes as persistent, high-amplitude scatterers in InSAR imagery therefore presents an immediate opportunity to unify ground displacement measurements from InSAR across continents, while avoiding the implicit assumptions, additional costs, and ongoing fieldwork required when connecting InSAR measurements to other geodetic infrastructures.

The integration of InSAR and VLBI necessitates a small paradigm shift in VLBI instrument operations (i.e., pointing telescopes toward, rather than away from, the satellite-radar beam), which requires international cooperation to fully realize. The proof-of-concept experiments described herein are intended to initiate international adoption of this new approach, which has arisen in light of advances and expansion of SAR technology. We use two common VLBI telescope types to validate different modes of tracking SAR satellites, while ensuring protection of telescopes' delicate electronics from the illuminating radar. We find that tracking is easily automated and implemented alongside existing, ongoing VLBI observation schedules and thus demonstrate that this existing telescope infrastructure is well suited to unify InSAR-derived ground displacements across continents within an absolute geocentric reference frame. This represents the first discussion of implementing satellite-radar measurements on a truly global scale.

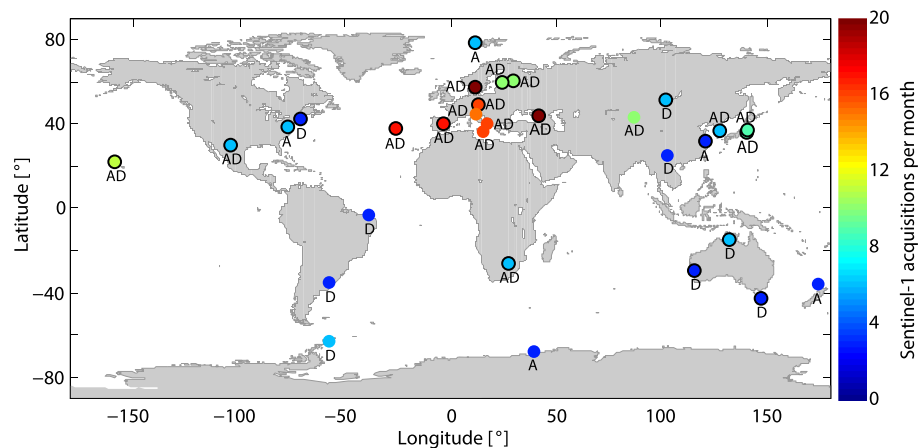


Figure 1. The global network of the International Very Long Baseline Interferometry Service telescopes. Circles with black outlines indicate sites where next-generation VLBI Global Observing System instruments will be, or are already, located. All telescopes are imaged by the European Space Agency synthetic aperture radar satellite constellation Sentinel-1 in either (or both) a south to north ascending orbit (labeled A) or a north to south descending orbit (labeled D) at a repeat frequency between 1 and 12 days.

2. Concept and Method

Four telescopes from the global VLBI network (Figure 1) were used to test tracking of Sentinel-1 over a 3-month trial period. This includes the two most common types of telescope of the future VLBI Global Observing System (VGOS: Hase & Pedreros, 2014) network: 12-m-diameter COBHAM Satcom Patriot Products instruments (Lovell et al., 2013; Hobart, Hb; Katherine, Ke; and Yarragadee, Yg, located in Australia) and a 13.2-m-diameter MT Mechatronics instrument (Onsala, Oe, located in Sweden).

2.1. Implementing Telescope Tracking Modes

Two approaches to SAR satellite tracking were tested: Telescopes either were pointed in a single, static orientation (fixed azimuth and elevation angle) toward the overpassing SAR satellite or were steered to track the SAR satellite overpass using time-tagged orientation parameters. For a given telescope and SAR satellite orbit, orientation parameters were calculated based on the location of the telescope (geodetic coordinates of latitude, longitude, and ellipsoidal height) and satellite orbital information derived from up-to-date two-line element files (Hoots & Roehrich, 1980). When not in use for geodesy, astrometry, or SAR satellite tracking, VLBI telescopes are stowed in a baseline position to reduce gravity sag (cf. Bergstrand et al., 2019) and mechanical stress on the mountings. The Australian telescopes are stowed pointing in a near-zenith direction (azimuth 0° , elevation angle 89°), whereas the Swedish Oe telescope is stowed close to horizon (azimuth 0° , elevation angle 0°) or near zenith during heavy storms.

Tracking SAR satellites is easily integrated alongside ongoing commitments of the global VLBI network to geodesy and astrometry, in which telescopes observe the arrival times of radio emissions from extragalactic quasars to determine and connect the terrestrial and celestial reference frames (e.g., Schuh & Behrend, 2012; Sovers et al., 1998). These observations are performed simultaneously at two or more telescopes on the Earth's surface and are coordinated by international collaboration via the IVS (International VLBI Service for Geodesy and Astrometry: Nothnagel et al., 2017; Schuh & Behrend, 2012). Coordinated VLBI observation sessions occur ~ 200 times per year, usually lasting 24 hr, and during which each telescope follows a sequence of 300 to 700 observation “scans,” pointing to a specific extragalactic target and recording data for a predefined observation period (between 30 and 300 s). Prior to observation sessions, the IVS issues a schedule to VLBI telescope operators, which is used to produce a sequence of commands enabling automated operation of antenna steering, signal chains, and sampler configuration for recording of the data.

If a SAR satellite overpass coincides with an IVS observation session, the scan(s) coincident with the overpasses can be overwritten and replaced with the orientation parameters of the radar satellite. Including steering, this corresponds to only one to two scans of the original IVS schedule being missed. Short breaks in

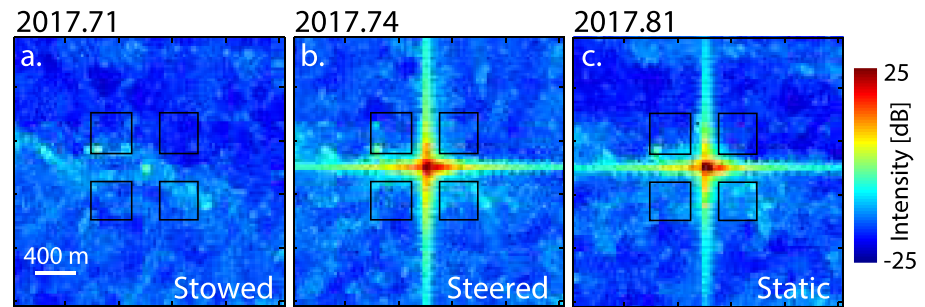


Figure 2. Synthetic aperture radar intensity imagery for different telescope tracking modes. Results are for telescope Yarragadee (Yarragadee, Australia) showing (a) the telescope stowed in the near-zenith stowed position and the impulse response observed when tracking Sentinel-1A via (b) steered and (c) static orientations. Black windows show the region used to calculate the background “clutter.” Images are in radar co-ordinates.

typical 24-hr observation sessions are shown not to significantly degrade results (Iles et al., 2017), and given the large number of scans per day (typically > 500 per station), we deem this to be entirely acceptable. In the future, the next-generation VGOS will use faster-slewing telescopes and short on-source times (Petrachenko et al., 2009) to double the number of scans per station, with at least two observations per minute per telescope. This will further reduce any impact of missing scans during SAR satellite overpasses until complete automation can be achieved via the dynamic observing concept (Iles et al., 2017; Lovell et al., 2013) and direct implementation of SAR tracks within session scheduling.

2.2. Comparing Telescope Tracking Modes

The two modes of telescope tracking (static vs. steered) can be compared to the baseline setup by evaluating the “brightness” of the reflection from the telescope in coregistered SAR intensity imagery (Figure 2). To act as a persistent scatterer in SAR imagery, the telescope must provide a high-intensity radar reflection that is clearly differentiable from the backscatter response of surrounding scatterers, the so-called clutter. The relative “brightness” of the reflection is quantified as a signal-to-clutter ratio (SCR: Ferretti et al., 2007; Garthwaite, 2017; Parker et al., 2017). The SCR measures the ratio between the integrated point target energy measured in the target window (the telescope) and that arising from the average background “clutter.”

Here, SCRs were calculated using a target window of 3×3 pixels located at the center of each telescope’s impulse response. The background clutter in the SAR imagery was then calculated using four quadrants (black squares in Figure 2) that shoulder the side lobes of the telescope impulse response. This approach provides the most representative measure of clutter and avoids bias associated with choosing arbitrary windows containing the lowest clutter in the region surrounding the target (cf. Garthwaite, 2017). For reference we also examined the phase stability of other man-made structures in the SAR imagery that yield “bright” reflections ($SCR > 10$ dB) (see grey circles in Figure 3).

2.3. Unification of InSAR Velocities

A worked example demonstrating how to utilize VLBI telescopes as persistent scatterers in InSAR imagery and thus unify InSAR-derived velocities intercontinentally for the Oe and Yg telescopes and a set of simulated InSAR-derived velocities is shown in the Supporting Information. Application to measured InSAR-derived velocities is reliant upon a long-enough time series of observation epochs in order to attempt to determine any reliable InSAR rates. Accurately determining the error on the InSAR-measured velocities at the telescopes is further reliant upon an assessment of the phase stability of the scatterer over the time series (see details in Garthwaite, 2017).

The primary geodetic use of VLBI aims to determine the time series of geocentric Cartesian coordinates at the invariant point of the telescopes, which is the intersection of axes that is not directly observable so has to be determined indirectly by local land-surveying techniques (cf. Dawson et al., 2007; Lösler et al., 2013). The geocentric Cartesian velocities are computed from these invariant point coordinates using time series analysis (cf. Altamimi et al., 2016). As such, the question may arise as to how the SAR reflection point on the telescope relates to the invariant point. We contend that this does not affect our technique, as we are

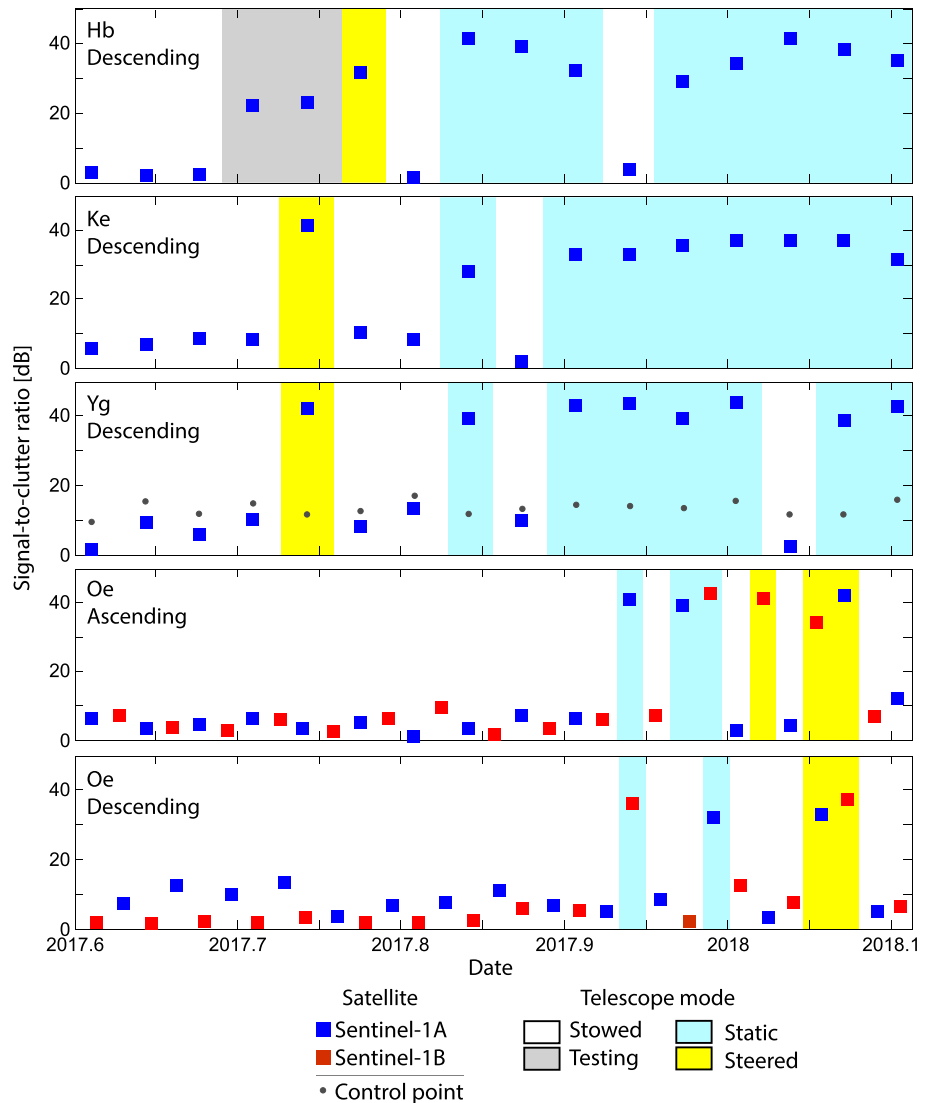


Figure 3. Time series of signal-to-clutter ratios at four Very Long Baseline Interferometry telescopes. Hobart, Katherine, and Yarragadee are located in Australia. Onsala is located in Sweden. The initial testing phase at Hobart was undertaken to ensure protection of receiver electronics. The ground control point shown for Yarragadee is a man-made building situated ~300 m from the telescope.

concerned with the geodetic velocities of the telescope structure. Fundamentally, the geometry of the telescope is deliberately left unchanged. As such, so long as the telescope is pointed consistently to each SAR satellite, it becomes immaterial as to exactly where the SAR reflection originates from on the telescope.

3. Results

3.1. Static Versus Steered Tracking

Tracking SAR satellites across the global VLBI network requires a mode of steering that is suitable for all telescopes. In testing different telescope types, we found that new-generation telescopes (e.g., Oe) can directly read satellite two-line element file information available in the telescope operation systems and use this to seamlessly implement either automated static or steered tracking of overpassing SAR satellites. Conversely, telescopes operating with “standard” IVS antenna control software (Hb, Ke, and Yg) first require orientation parameters to be calculated from the two-line element files externally, using a platform such as the open-access Systems Tool Kit modeling environment (<http://www.agi.com/products/stk/>; e.g., Parker

et al., 2017). These telescopes do not necessarily enable automatic steered tracking of satellites (Hellerschmied et al., 2018; Plank et al., 2017). Instead, steered tracking of the Australian telescopes requires manual implementation using a time-tagged list of discrete azimuth and elevation angle orientations at 1-s intervals, which is loaded into the antenna's control system. Static tracking of SAR satellites can, more simply, be treated in a similar way as a scan to a radio source. Consequently, static mode (single azimuth and elevation angle) tracking is more generally suited to different telescope types. This static approach is very straightforward to implement into existing IVS observing commitments and automated antenna orientation sequences, requiring only minor alterations to current operating procedures.

Our first evaluation of SAR intensity imagery demonstrates that, when stowed in the baseline setup (near zenith for Hb, Ke, and Yg and horizon for Oe), VLBI telescopes do not act as bright reflectors for Sentinel-1 SAR (SCR ~ 0 ; Figures 2 and 3). However, both static and steered tracking of the Sentinel-1 satellites provides the desired high-amplitude impulse response (Figure 2) and results in comparable SCR values that are above 30 dB (Figure 3), the threshold used for SAR calibration and validation purposes (Freeman, 1992). Any variability in the SCRs over time (Figure 3) is due to changes in the orientation of neighboring ground infrastructure (e.g., other telescopes) and environmental factors (e.g., changes in moisture) as demonstrated by the example of time series of a control point (man-made building) at Yg, which shows comparable variations in SCR over time as the Yg telescope (variations within 4 dB: gray circles in Figure 3).

SCRs, observed when tracking Sentinel-1 in either static or steered mode, are considerably larger than those observed in tests with 1-m trihedral CRs (13 dB for Sentinel-1B: Parker et al., 2017), due to the larger size of the target (12-m or 13.2-m diameter). As both tracking modes yield calibration-grade SCRs, they are both equally valid for the proposed purpose of global unification of InSAR time series. This finding is crucial to the feasibility of implementing this technique at all telescopes in the global VLBI network (Figure 1). Static tracking of Sentinel-1 is now fully automated at telescopes Hb, Ke, and Yg and will continue indefinitely.

3.2. Protection of Receiver Electronics

Radio astronomical telescopes are designed to observe low-power radiation from extragalactic quasars. Received signals directly pass from the antenna feed to a sensitive low-noise amplifier (LNA) in the receiver, which—by default—is not protected against damaging, high-power radio-frequency interference (RFI). The damage threshold levels for S/X-band (Yg, Ke) and new VGOS broadband (Hb, Oe) VLBI receivers are comparable to the peak power levels of SAR satellites, with the VGOS damage level (-40 dB/(W/m²): Hase et al., 2016) only marginally above the maximum power flux density of SAR satellites (-45 dB/(W/m²): NASA, 2011). Protection of LNAs from the illuminating satellite radar is the only *caveat emptor* of deliberately using VLBI telescopes as SAR targets, and consequently during these experiments, measures were taken to ensure protection of the telescopes' electronics.

Regardless of the necessity to implement protection measures for the integration of InSAR and VLBI, protection of telescope electronics is beneficial (and in some cases essential) for avoiding ambient levels of high RFI. Multiple mechanisms are available, including avoidance of the satellite beam (modus operandi for current VLBI activities), electronic or physical protection of the LNA, or turning off the LNA during a SAR satellite overpass. In essence, VLBI telescope operators would normally want to avoid SAR satellites, whereas we are recommending they target them to achieve this previously unforeseen new and additional application for VLBI telescopes.

Electronic LNA protection via diode limiters is a default component of receiver chains at all telescopes tested in these experiments, as all operate in high-RFI areas. In these cases, SAR satellites can be tracked without damaging the LNAs. The installation of protective diodes at other telescopes will depend on the characteristics of the individual LNA (Hase et al., 2016) but potentially poses a loss in antenna sensitivity.

Additional physical LNA protection was implemented at the Oe telescope by installing a blocking mechanism consisting of material that is nonpermeable for the radar frequency (~ 5.404 GHz), in this case, metallic foil. The blocking mechanism prevents damage to the receiver during SAR satellite tracking and from other RFI when the telescope is stowed. Consequently, a prototype multipurpose, automated blocking system is under development for installation at Oe to facilitate automated long-term SAR tracking operations. An alternative option is to install a remote switch to power off the LNA completely during a SAR track, as

successfully tested and installed at Yg during observations of RadioAstron (Litvinov et al., 2017). In this instance, it must be ensured that switching off the LNAs during a VLBI experiment does not cause undesired jumps in the calibration signals or in the recorded data.

Another approach to LNA protection, tested during our initial experiments (see gray panel in Figure 3), is to slightly off-point the VLBI antenna during the SAR overpasses. However, a balance needs to be reached to achieve an acceptable power in the SCR (30 dB for calibration purposes; Freeman, 1992). During testing at Hb, the telescope was off-pointed by up to 2° , reducing the SCR to ~ 20 dB, below our accepted threshold.

Rapidly rising numbers of active SAR satellites, now including commercially launched SAR “microsatellites,” plus more sophisticated radar modes, mean that it will continue to become increasingly difficult for VLBI operators to simply avoid telescopes intersecting satellite-radar beams. Each of the protection mechanisms described above is entirely viable for telescopes across the global VLBI network, having been successfully implemented at the two most commonly used types of telescopes during our experiments. An assessment of the observed satellite and each tracking antenna will determine the mechanism that is most suitable on a case-by-case basis. Currently, a new generation of VLBI telescopes is in the construction phase as international VLBI operations transition to the VGOS in line with requirements of the next-generation global geodetic observing system (GGOS; Plag & Pearlman, 2009). We propose that the international community therefore looks now to implement automated LNA protection mechanisms, since physical changes to the receiver will be easier to devise during commissioning, construction, and installation, rather than to retrofit.

4. Outlook and Prospects

Advances in the use of InSAR to understand Earth-system dynamics are occurring in line with the recent “step change” in the provision and consistency of satellite-radar data (e.g., Elliott et al., 2016). Inevitably, InSAR applications will expand to a global scale, but to fully realize this global potential first requires a framework to unify intercontinental InSAR measurements within a consistent geocentric reference frame using absolute geodetic methods. The existing international network of VLBI telescopes is herein shown to be an unexploited, yet well-suited, link to achieve this vision.

Globally unified InSAR measurements have unique potential to deliver a complete and consistent assessment of the land component of relative sea-level change. This phenomenon is globally ubiquitous (Nicholls & Cazenave, 2010), impacting upon growing coastal populations and records of sea-level change (Raucoules et al., 2013; Wöppelmann et al., 2013), but remains little studied (Bekaert et al., 2017). Similarly, the spatial resolution, coverage, and accuracy of InSAR measurements are now sufficient to assess the fundamental mechanics of the way in which continents deform (Elliott et al., 2016). Utilizing a unified set of global measurements expands the field of view from discrete studies of faults or plate boundaries (Walters et al., 2016), to the scale of entire plates, constraining the distribution and rate of strain accumulation in Earth’s crust at a level of detail simply unachievable by ground-based methods. Strain rates (predominantly estimated from cGNSS) are a key input to global forecasts of earthquake hazard (Kreemer et al., 2014), and advances to these estimates from globally unified InSAR will impact most considerably in regions where cGNSS coverage is limited (Elliott et al., 2016).

From another perspective, integrating InSAR and VLBI expands the scope of satellite radar to contribute to regularly updating geodetic coordinates and datums (as proposed by Fuhrmann et al., 2018), the significance of which permeates all measurements of global change. The most precise of these global coordinate frames is the ITRF, which relies heavily on repeated local surveying ties between co-located space geodetic techniques (e.g., VLBI, Satellite Laser Ranging, and/or cGNSS). Local ties are typically measured by land surveying (Dawson et al., 2007; Lösler et al., 2013, 2016; Sarti et al., 2004), but discrepancies between the surveyed ties and space geodetic results have limited improvements to the ITRF (Altamimi et al., 2016, 2011). Co-location of SAR CRs with VLBI telescopes (as recently implemented at Yg) also bears potential to independently verify local ties, allowing the land-surveying vector to be compared to the projected differential vector measured by InSAR.

Initiation of these new modes of VLBI-InSAR activities requires a modest paradigm shift in telescope operations and international cooperation to be fully realized yet in reality involves only simple additions to IVS

VLBI operations that can be easily implemented and automated by all telescope operators. Such advances in approaches to the integration of relative satellite-radar measurements with absolute geodetic methods comprise a first step toward using InSAR on a truly global scale.

Acknowledgments

All data used in this study are publicly available. SAR data were accessed via the Copernicus Open Access Hub (<https://scihub.copernicus.eu/dhus/#/home>) and processed using the open-access European Space Agency Sentinel Application Platform Toolbox (<http://step.esa.int/main/toolboxes/snap/>). International Terrestrial Reference Frame 2014 geodetic coordinates and linear site velocities were accessed from the ITRF website (http://itrf.ensg.ign.fr/ITRF_solutions/2014/ITRF2014.php).

Geodetic VLBI operations at the University of Tasmania, Australia, are supported through the AuScope initiative, contracted through Geoscience Australia. AuScope Ltd is funded under the National Collaborative Research Infrastructure Strategy, an Australian Commonwealth government program. We thank Ulf Kylanfall for supporting the experiments using Oe. L. McCallum and A. Parker are the recipients of **Australian Research Council Discovery Early Career Researcher Awards** (projects P0025355 and DE190101389) funded by the Australian Government. This research was also supported partially by the Australian Government through the Australian Research Council's *Linkage Projects* funding scheme (project LP140100155).

References

- Altamimi, Z., Collilieux, X., & Métivier, L. (2011). ITRF2008: An improved solution of the International Terrestrial Reference Frame. *Journal of Geodesy*, *85*, 457–473. <https://doi.org/10.1007/s00190-011-0444-4>
- Altamimi, Z., Rebischung, P., Métivier, L., & Xavier, C. (2016). ITRF2014: A new release of the International Terrestrial Reference Frame modelling nonlinear station motions. *Journal of Geophysical Research: Solid Earth*, *121*, 6109–6131. <https://doi.org/10.1002/2016JB013098>
- Bekaert, D. P. S., Hamlington, B. D., Buzzanga, B., & Jones, C. E. (2017). Spaceborne synthetic aperture radar survey of subsidence in Hampton Roads, Virginia (USA). *Scientific Reports*, *7*(1), 14752. <https://doi.org/10.1038/s41598-017-15309-5>
- Bergstrand, S., Herbertsson, M., Rieck, C., Spetz, J., Svantesson, C. G., & Haas, R. (2019). A gravitational telescope deformation model for geodetic VLBI. *Journal of Geodesy*, *93*(5), 669–680. <https://doi.org/10.1007/s00190-018-1188-1>
- Bock, Y., Wdowinski, S., Ferretti, A., Novali, F., & Fumagalli, A. (2012). Recent subsidence of the Venice Lagoon from continuous GPS and interferometric synthetic aperture radar. *Geochemistry, Geophysics, Geosystems*, *13*, Q03023. <https://doi.org/10.1029/2011GC003976>
- Copernicus Space Component Mission Management Team (2017). Sentinel High Level Operations Plan. *Tech. Rep. COPE-SIOP-EOPG-PL-0020*, European Space Agency, Paris.
- Dawson, J. M., Sarti, P., Johnston, G. M., & Vittuari, L. (2007). Indirect approach to invariant point determination for SLR and VLBI systems: An assessment. *Journal of Geodesy*, *81*, 433–441. <https://doi.org/10.1007/s00190-006-0125-x>
- Dheanathayalan, P., Small, D., Schubert, A., & Hanssen, R. F. (2016). High-precision positioning of radar scatterers. *Journal of Geodesy*, *90*(5), 403–422. <https://doi.org/10.1007/s00190-015-0883-4>
- Elliott, J. R., Walters, R. J., & Wright, T. J. (2016). The role of space-based observation in understanding and responding to active tectonics and earthquakes. *Nature Communications*, *7*, 13844. <https://doi.org/10.1038/ncomms13844>
- Ferretti, A., Savio, G., Barzaghi, R., Borghi, A., Musazzi, S., Novali, F., et al. (2007). Submillimeter accuracy of InSAR time series: Experimental validation. *IEEE Transactions on Geoscience and Remote Sensing*, *45*, 1142–1153. <https://doi.org/10.1109/TGRS.2007.894440>
- Finnegan, N. J., Pritchard, M. E., Lohman, R. B., & Lundgren, P. R. (2008). Constraints on surface deformation in the Seattle, WA, urban corridor from satellite radar interferometry time-series analysis. *Geophysical Journal International*, *174*, 29–41. <https://doi.org/10.1111/j.1365-246X.2008.03822.x>
- Freeman, A. (1992). SAR calibration: An overview. *IEEE Transactions on Geoscience and Remote Sensing*, *30*, 1107–1121. <http://doi.org/10.1109/36.193786>
- Fuhrmann, T., Garthwaite, M., Lawrie, S., & Brown, N. (2018). Combination of GNSS and InSAR for future Australian datums, In proceedings of International Global Navigation Satellite Systems Association Symposium 2018, University of New South Wales, Australia, 7-9 February 2018.
- Galloway, D. L., Hudnut, K. W., Ingebritsen, S. E., Phillips, S. P., Peltzer, G., Rogez, F., & Rosen, P. A. (1998). Detection of aquifer system compaction and land subsidence using interferometric synthetic aperture radar, Antelope Valley, Mojave Desert, California. *Water Resources Research*, *34*, 2573–2585. <https://doi.org/10.1029/98WR01285>
- Garthwaite, M. C. (2017). On the design of radar corner reflectors for deformation monitoring in multi-frequency InSAR. *Remote Sensing*, *9*, 648. <https://doi.org/10.3390/rs9070648>
- Goldstein, R. M., Engelhardt, H., Kamb, B., & Frolich, R. M. (1993). Satellite radar interferometry for monitoring ice sheet motion: Application to an Antarctic ice stream. *Science*, *262*(5139), 1525–1530. <http://doi.org/10.1126/science.262.5139.1525>
- Hase, H., & Pedreros, F. (2014). The most remote point method for the site selection of the future GGOS network. *Journal of Geodesy*, *88*(10), 989–1006. <https://doi.org/10.1007/s00190-014-0731-y>
- Hase, H., Tornatore, V., & Corey, B. (2016). How to register a VGOS radio telescope at ITU and why it is important. *Proc IVS 2016 General Meeting "New Horizons With VGOS"* NASA/CP-2016-219016, 65–68.
- Hellerschmied, A., McCallum, L., McCallum, J., Sun, J., Böhm, J., & Cao, J. (2018). Observing APOD with the AuScope VLBI array. *Sensors*, *18*, 1587. <https://doi.org/10.3390/s18051587>
- Hoots, F., & Roehrich, R. (1980). Spacetrack report number 3: Models for propagation of NORAD element sets. *Tech. Rep., US Air Force Aerospace Defence Command, Colorado Springs*.
- Hussein, E., Wright, T. J., Walters, R. J., Bekaert, D. P. S., Lloyd, R., & Hooper, A. J. (2018). Constant strain accumulation rate between major earthquakes on the North Anatolian Fault. *Nature Communications*, *9*, 1392. <https://doi.org/10.1038/s41467-018-03739-2>
- Iles, E. J., McCallum, L., Lovell, J. E. J., & McCallum, J. N. (2017). Automated and dynamic scheduling for geodetic VLBI—A simulation study for AuScope and global networks. *Advances in Space Research*, *61*, 962–973. <https://doi.org/10.1016/j.asr.2017.11.012>
- Keen, K. M. (1983). Use of radio telescopes or satellite earth station antennas as ultra-high scattering cross-section calibration targets for spaceborne remote sensing radars. *Electronics Letters*, *19*, 225–226. <http://doi.org/10.1049/el:19830155>
- Kreemer, C., Blewitt, G., & Klein, E. C. (2014). A geodetic plate motion and Global Strain Rate Model. *Geochemistry, Geophysics, Geosystems*, *15*, 3849–3889. <https://doi.org/10.1002/2014GC005407>
- Litvinov, D. A., Rudenko, V. N., Alakoz, A. V., Bach, U., Bartel, N., Belonenko, A. V., et al. (2017). Probing the gravitational redshift with an Earth-orbiting satellite. *Physics Letters A*, *382*(33), 2192–2198. <https://doi.org/10.1016/j.physleta.2017.09.014>
- Löslér, M., Haas, R., & Eschelbach, C. (2013). Automated and continual determination of radio telescope reference points with sub-mm accuracy: Results from a campaign at the Onsala Space Observatory. *Journal of Geodesy*, *87*(8), 791–804. <https://doi.org/10.1007/s00190-013-0647-y>
- Löslér, M., Haas, R., & Eschelbach, C. (2016). Terrestrial monitoring of a radio telescope reference point using comprehensive uncertainty budgeting. *Journal of Geodesy*, *90*(5), 467–486. <https://doi.org/10.1007/s00190-016-0887-8>
- Lovell, J. E. J., McCallum, J. N., Reid, P. B., McCulloch, P. M., Baynes, B. E., Dickey, J. M., et al. (2013). The AuScope geodetic VLBI array. *Journal of Geodesy*, *87*(6), 527–538. <https://doi.org/10.1007/s00190-013-0626-3>
- Mahapatra, P., van der Marel, H., van Leijen, F., Samiei-Esfahany, S., Klees, R., & Hanssen, R. (2018). InSAR datum connection using GNSS-augmented radar transponders. *Journal of Geodesy*, *92*(1), 21–32. <https://doi.org/10.1007/s00190-017-1041-y>

- Mahapatra, P. S., Samiei-Esfahany, S., van der Marel, H., & Hanssen, R. F. (2014). On the use of transponders as coherent radar targets for SAR interferometry. *IEEE Transactions on Geoscience and Remote Sensing*, *52*, 1869–1878. <https://doi.org/10.1109/TGRS.2013.2255881>
- Massonnet, D., & Feigl, K. L. (1998). Radar interferometry and its application to changes in the Earth's surface. *Reviews of Geophysics*, *36*, 441–500. <https://doi.org/10.1029/97RG03139>
- Meadows, P. (2000). The use of ground receiving stations for ERS SAR quality assessment. In Proceedings of SAR Workshop: CEOS Committee on Earth Observing Satellites; Working Group on Calibration and Validation, held 26–29 October 1999, ESA Publication SP-450, 525–530.
- NASA (2011). Potential damage to RAS sites by EESS (active), (SFCG Action Item 30/8), *SFCG-31, San Francisco, CA, USA, 7–15 June 2011*. <https://www.sfcgonline.org/Public%20Documents/SF31-09DR1.pdf>
- Nicholls, R. J., & Cazenave, A. (2010). Sea-level rise and its impact on coastal zones. *Science*, *328*(5985), 1517–1520. <http://doi.org/10.1126/science.1185782>
- Nothnagel, A., Artz, T., Behrend, D., & Malkin, Z. (2017). International VLBI Service for Geodesy and Astrometry: Delivering high-quality products and embarking on observations of the next generation. *Journal of Geodesy*, *91*(7), 711–721. <https://doi.org/10.1007/s00190-016-0950-5>
- Parker, A. L., Featherstone, W. E., Penna, N. T., Filmer, M. S., & Garthwaite, M. C. (2017). Practical considerations before installing ground-based geodetic infrastructure for integrated InSAR and cGNSS monitoring of vertical land motion. *Sensors*, *17*, 1753. <http://doi.org/10.3390/s17081753>
- Petrachenko, W., Niell, A., Corey, B., Behrend, D., Schuh, H., & Wresnik, J. (2009). VLBI2010: Next generation VLBI system for geodesy and astrometry. In S. Kenyon, M. Pacino, & U. Marti (Eds.), *Geodesy for Planet Earth, International Association of Geodesy Symposia* (Vol. 136, pp. 999–1006). Berlin, Heidelberg: Springer. https://doi.org/10.1007/978-3-642-20338-1_125
- Plag, H.-P., & Pearlman, M. (2009). *Global Geodetic Observing System: Meeting the requirements of a global society on a changing planet in 2020*. Springer.
- Plank, L., Hellerschmied, A., McCallum, J., Bohm, J., & Lovell, J. (2017). VLBI observations of GNSS-satellites: From scheduling to analysis. *Journal of Geodesy*, *91*(7), 867–880. <https://doi.org/10.1007/s00190-016-0992-8>
- Raucoules, D., Le Cozannet, G., Wöppelmann, G., de Michele, M., Gravelle, M., Daag, A., & Marcos, M. (2013). High nonlinear urban ground motion in Manila (Philippines) from 1993 to 2010 observed by DInSAR: Implications for sea-level measurement. *Remote Sensing of Environment*, *139*, 386–397. <https://doi.org/10.1016/j.rse.2013.08.021>
- Sarti, P., Sillard, P., & Vittuari, L. (2004). Surveying co-located space-geodetic instruments for ITRF computation. *Journal of Geodesy*, *78*, 210–222. <https://doi.org/10.1007/s00190-004-0387-0>
- Schmidt, D. A., & Bürgmann, R. (2003). Time-dependent land uplift and subsidence in the Santa Clara valley, California, from a large interferometric synthetic aperture radar data set. *Journal of Geophysical Research*, *108*(B9), 2416. <https://doi.org/10.1029/2002JB002267>
- Schuh, H., & Behrend, D. (2012). VLBI: A fascinating technique for geodesy and astrometry. *Journal of Geodynamics*, *61*, 68–80. <https://doi.org/10.1016/j.jog.2012.07.007>
- Sovers, O. J., Fanselow, J. L., & Jacobs, C. S. (1998). Astrometry and geodesy with radio interferometry: Experiments, models, results. *Reviews of Modern Physics*, *70*, 1393. <https://doi.org/10.1103/RevModPhys.70.1393>
- Torres, R., Snoeij, P., Geudtner, D., Bibby, D., Davidson, M., Attema, E., et al. (2012). GMES Sentinel-1 mission. *Remote Sensing of Environment*, *120*, 9–24. <http://doi.org/10.1016/j.rse.2011.05.028>
- van't Klooster, C. G. M. (2011). About ground-station antennas as 'radar target' for P-band synthetic aperture radars in space. In *2011 IEEE International Symposium on Antennas and Propagation (APSURSI)* (pp. 3233–3236).
- Walters, R. J., Gonzalez, P. J., Hatton, E. L., Hooper, A. J., & Wright, T. J. (2016). Plate-scale measurement of interseismic strain from Sentinel-1. In AGU Fall Meeting Abstracts.
- Wöppelmann, G., Le Cozannet, G., de Michele, M., Raucoules, D., Cazenave, A., Garcin, M., et al. (2013). Is land subsidence increasing the exposure to sea level rise in Alexandria, Egypt? *Geophysical Research Letters*, *40*, 2953–2957. <https://doi.org/10.1002/grl.50568>
- Zakharov, A. I., Zherdev, P. A., Borisov, M. M., Sokolov, A. B., & van't Klooster, C. G. M. (2003). On the stability of large antennas as calibration targets. *Proc 2003 IEEE International Geoscience and Remote Sensing Symposium*, *7*, 4518–4520. <http://doi.org/10.1109/IGARSS.2003.1295566>